

Automatic Detection of Human's Lung Nodules Using an Optimal Gray Level Threshold

Hanan M. Amer, Hamdi A. A. Elmikati, Fatma E.Z. Abou-Chadi, Sherif S. Kishk and Marwa I. Obayya

Abstract—The objective of the paper is to present an automatic detection framework for the segmentation of human's lung and pulmonary nodule candidates (nodules, blood vessels) with high accuracy. The proposed framework is based on an automatic segmentation of the lungs followed by an automatic segmentation of the pulmonary nodules using a two-level thresholding technique based on an optimal gray level threshold incorporated with the morphological operations that lead to complete segmentation of lungs and good localized of the pulmonary nodule candidates. To assess the performance of the segmentation results, the proposed algorithm was applied to a number of standard Computed Tomographic (CT) images available through an early lung cancer action project (ELCAP) association. The applied images consists of 40 CT scans contains 320 region of interest (ROI). The results were compared with those obtained from other three previously published algorithms and showed that the proposed framework gives the highest accuracy and helps to increase the speed of the Computer-Aided Detection (CAD) systems.

Index Terms—Computer-aided detection, histogram thresholding, image preprocessing, region of interest, contrast enhancement, lung segmentation, nodule candidates detection.

1 INTRODUCTION

Lung nodules are masses of soft tissue located in the lung and can be detected using modern imaging techniques. They are one of the critical notifications to detect lung cancer [1],[2]. They take the oval or circle opacity in the chest Computed Tomographic (CT) scan images. There are classified on the basis of the internal texture, where they are subdivided into three types: solid, non-solid, and part-solid pulmonary nodules as illustrated in Fig.1 based on the appearance of lung parenchyma. It is complete obscure in case of solid nodules while it does not obscure the internal structure of lung parenchyma and appears as focal hazy nodule in case of non-solid nodules. In case of part-sold, it shows a wide range of intensity variation. Classification of Lung nodules can also be based on the external attachment [3]. These are juxta-vascular, well-circumscribed, and juxta-pleural as illustrated in Fig.2.

In the past few years, a number of Computer-Aided Detection (CAD) systems for the automated detection of small nodules from CT lung images have been developed [3],[4],[5],[6]. These systems are designed and developed to reduce the great effort aspirated by radiologist in interpreting the lung CT scans images of the large number of images and support them in making the decision. All CAD systems of lung nodules detection share a general framework of basic steps. These steps can be summarized in the following steps; image preprocessing, segmentation of human's lung, segmentation of pulmonary nodules candidate, finally the characterization and classification step which consists of feature extraction and selection step follow by reducing the false positive nodules detection using different classifier algorithms [4].

Lung segmentation is a common stage between all CAD systems where the accurate extraction of the lungs from the CT chest images is an essential step in the CAD systems. Previous techniques used previously in lung segmentation are based on intensity variation (thresholding methods),image region (merge region, split region, and the region growing techniques), and others that are based on the object texture, motion tracking, and edge detection [4],[5].

Having extracted the human's lung from the CT images, the next step is the extraction of pulmonary nodule candidate. Several techniques were utilized for nodule extraction [3],[4],[5]. Of these techniques are thresholding techniques [6]where the extraction of the nodule candidates is based on the intensity variation between the lung parenchyma and the nodule candidates. In addition to the shape-based techniques [7], template-matching-based techniques [8], morphological operations and filtering-based techniques [9],[10].According to clinical opinions of physicians, the blood vessels and pulmonary nodules are

- Hanan M. Amer is assistant teacher in department of electronics and communications, faculty of engineering, Mansoura University, Egypt. E-mail: hanan.amer@yahoo.com
- Hamdi A. A. Elmikati is professor in department of electronics and communications, faculty of engineering, Mansoura University, Egypt.
- Fatma E.Z. Abou-Chadi is professor in department electrical engineering, faculty of engineering, the British University in Egypt.
- Sherif S. Kishk is Assistant Professor in department of electronics and communications, faculty of engineering, Mansoura University, Egypt.
- Marwa I. Obayya is Assistant Professor in department of electronics and communications, faculty of engineering, Mansoura University, Egypt.

presented in the CT scan image as having lower contrast values and higher gray values[11].This intensity variation leads to the adoption of the thresholding techniques. Accurate extraction of pulmonary nodule candidates can be obtained if an appropriate gray level threshold was chosen.

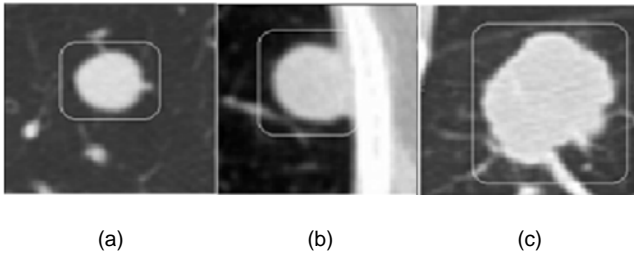


Fig 1: (a) The solid pulmonary nodules, (b) non-solid pulmonary nodules, and (c) part-solid pulmonary nodules.

In the present work, an automatic detection framework has been proposed. Using an optimal gray level threshold for real time segmentation of human's lung and pulmonary nodule candidates, it has been possible to identify nodules of different types including: solid, non-solid, part-solid, juxta-vascular, well-circumscribed, and juxta-pleural pulmonary nodules and blood vessels. It will be shown that the application of a bi-level thresholding technique with an optimal threshold lead to an accurate extraction of pulmonary nodules of any type of size up to 30 mm. The paper is organized as follows: Section 2 presents the applied images. Section 3 describes the proposed framework and the performance evaluation. Conclusion is summarized in Section 4.

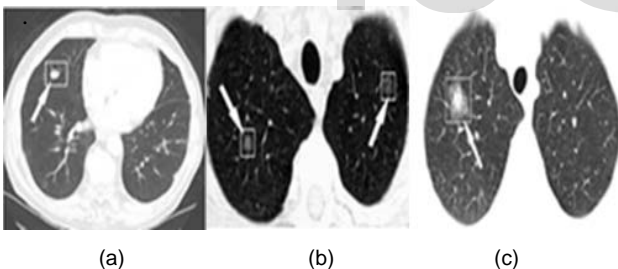


Fig 2: (a) the well-circumscribed pulmonary nodules, (b) juxta-pleural pulmonary nodules, and (c) juxta-vascular pulmonary nodules.

2 THE APPLIED IMAGES

The proposed framework has been applied to 40 CT scans containing 320 regions of interest (ROI) available by the early lung cancer action project (ELCAP) association [12].The first release of this database was produced in December 2003 and was in collaboration with the research teams belonging to VIA and ELCAP associations. The resolution of this database images is $0.76 \times 0.76 \times 1.25$ and they are ready in format of Digital Images and Communication in Medicine (DICOM).Only nodules larger than 3 mm were considered in this work. Fig.3 shows atypical example of the unprocessed chest CT images.

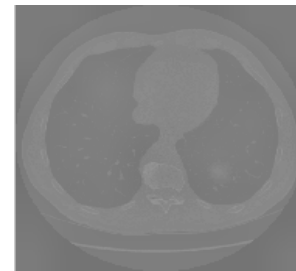


Fig 3: A typical example of CT lung image from ELCAP database.

3 THE PROPOSED FRAMEWORK

Fig. 4 shows a schematic diagram for the proposed framework. It consists of an image preprocessing step for image contrast enhancement and noise reduction. Then the automatic segmentation system that aims to extract the human's lung area followed by extracting the pulmonary nodule candidates in the digital CT images.

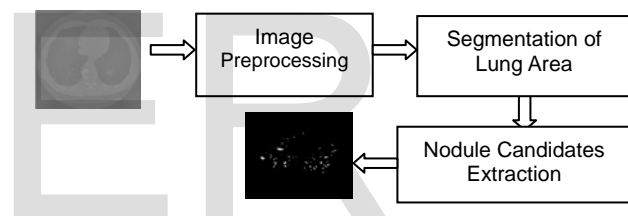


Fig 4: Schematic diagram of the proposed framework

3.1 Image Preprocessing

The reduction of the negative side effects of x-ray radiation on human health that is used in human examination by CT scan is associated with the reduction of radiation dose during CT examinations but this lead to get low-resolution and unsharp images, in the same time reduced the image quality, and then the low ability of distinguishing between normal and abnormal lung tissues. On the other hand, the process of human examination by CT scan itself is accompanied by the exposure of images to the noise from different sources including the patient, the CT scan system and the surrounding environment. This noise reduce the image quality which affects the process of diagnosis using these images. All of the above makes preprocessing of CT chest image is a significant part of the proposed recognition systems. The preprocessing of CT chest image is made up of two main steps; starting by enhancing the image contrast followed by reducing the noise in the CT chest image.

3.1.1 Image Contrast Enhancement

Contrast enhancement of CT scan images causes enhancement syndromes diagnosis, increases the accuracy of diseases detection and leads to accurate detect of smaller

features and components of the CT scan images which give the physician the chance to execute a healthier treatment for the patient [19]. Hence, the next step in the present work is to conduct a comparative study of four image contrast enhancement techniques; histogram equalization [13], adaptive Histogram Equalization [14-15], Gamma correction [16], and anovel Image Size Dependent Normalization Technique (ISDNT) [17]. The four image contrast enhancement techniques were applied to CT chest images. The visual comparison of the contrast enhanced images using the four techniques showed that the ISDNT technique gives the best results. Fig.5 shows the resulted contrast enhanced images of the four techniques.

• **The Image Size Dependent Normalization Technique (ISDNT)**

A brief description of the ISDNT technique is presented in this subsection. ISDNT does not need any transformation process and can be applied directly in time domain. The enhancement of image contrast is based on the image size and the enhancement variable (K). K is the average of the input image and is calculated using the following equation:

$$K = \frac{\sum_{i=1}^i \sum_{j=1}^j x(i, j)}{m \times n} \tag{1}$$

where (x) is the original image. The image contrast is enhanced using the following equation [17]:

$$EI = \frac{[x - \min(x)] \times e^K}{[\max(x) - \min(x)]} \tag{2}$$

where(K) is the enhancement variable of Eq. (1), (min) is the minimum pixel intensity value of input image,(max) is the maximum pixel intensity value of input image, and (EI) is represent the enhanced contrast image. Fig.6shows a schematic diagram for the steps of ISDNT.

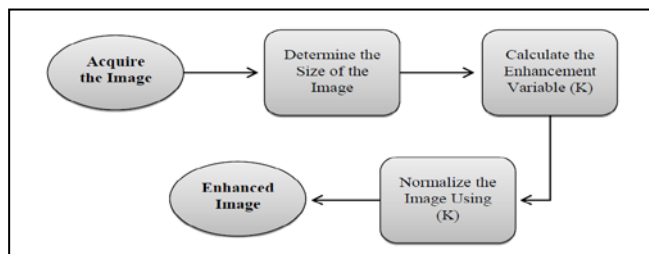


Fig 6: The INSDT technique steps, (Quoted from [17]).

3.1.2 Denoising of the CT Lung Images

Artifacts decrease of the quality of CT images. Therefore, the second step of preprocessing the CT image is image denoising. A previous study [20] compared the performance of six image denoising techniques: average filter [18], weighted average filter [18], Gaussian filter [18], median filter [18], Wiener filter [19], and wavelet filter [19] and concluded that the Wiener filter gives the best results. Fig.7 shows an example of a denoised image using Wiener filter.

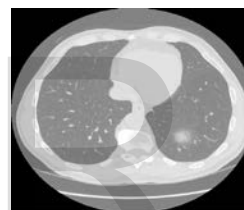


Fig7: A denoised CT lung image.

3.2 Lung Segmentation

Having preprocessing and denoised the CT lung images, the next step is to extract the human lungs area from CT chest images. The proposed algorithm of human lungs segmentation is presented in Fig.8. The first step is to calculate the optimal gray-level threshold as follows.

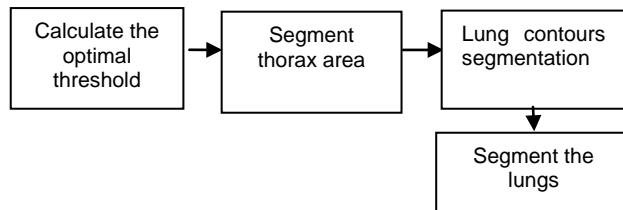


Fig 8: Segmentation steps of human lungs segmentation.

A diagonal gray-level histogram was constructed using the diagonal pixels intensity of all CT chest images of a complete scan. The resulted histogram was found to have three clear peaks as shown in Fig.9 and Fig.10. All CT chest scan images have this common property. These peaks represent the following; peak p1is formed from black background pixels intensity, peak p2is formed from the pixels of low intensity representing the external region that surrounds the thorax area and the internal parenchyma of lung, and peak p3is formed from the pixels of high intensity which represent blood vessels, bones of the rib cage, heart, and pulmonary nodules [11]. Accordingly, the choice

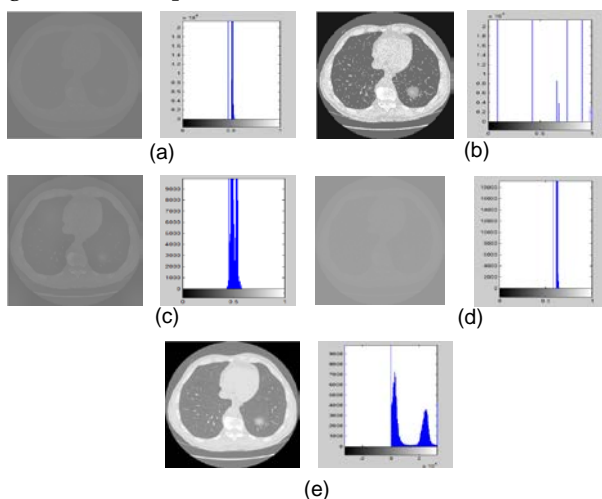


Fig 5: The raw CT chest image and the results obtained using the four contrast enhancement algorithms. (a) The raw chest image, (b) histogram equalized image (c) adaptive histogram equalized image, (d) gamma corrected image, and (e) INSDT image

of a gray-level point that divides the distance between the second and third peaks equally as an optimal gray-level threshold can be used to extract the lung area and then extract the pulmonary nodule candidates accurately. The optimal gray-level threshold is calculated according to the following equation;

$$L = (p_2 + p_3)/2. \quad (4)$$

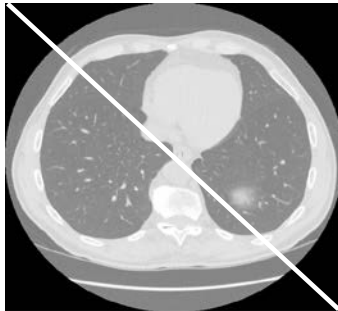


Fig 9: The location of pixels composing the diagonal gray-level histogram.

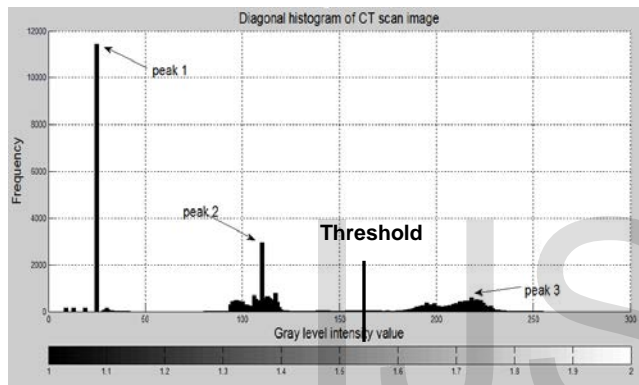


Fig 10: The diagonal gray-level histogram of CT scan .images.

The next step is to apply the morphological operations to segment the thorax area from background in each CT image then segment lungs within thorax and to avoid the loss of juxta-pleural nodules in order to obtain the two lungs from the CT chest image [21],[22],[23],[24].

3.2.1 Segment the Thorax from Background

To extract the human lungs area from the CT chest images, the thorax area must be first extracted. The thorax extraction includes the removal of each image component external to the chest area such as the surface on which patient lie on it as illustrated in Fig. (11.a). First, the bi-level thresholding technique was applied to obtain a binary image as shown in Fig. (11.b). The resulted binary image has the lung holes black area so this area needs to be filled to get a complete white thoracic area by using the filling morphological operations. In order to remove any unwanted pixels that exists in the black background pixels a median filter of size 15*15 was utilized to eliminate noise in the binary images. Examples of a filled and filtered image is shown in Fig. (11.c) and Fig. (11.d). Finally, the last step is to multiply the resulted binary image with a preprocessing gray level image to extract the thorax area from the background in the CT chest images. Fig. (11.e) shows the resulted the thoracic area.

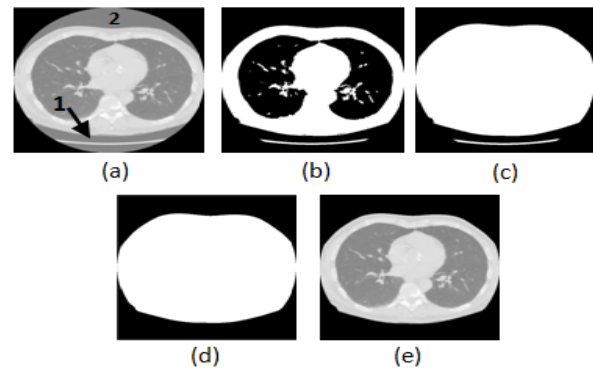


Fig 11: Results The preprocessed image, (d)

3.2.2 Segment the Lungs within the Thorax

The goal of this step is to separate human lungs area from the thoracic area where the thoracic area can be divided into three components: two lungs region, fat, and other tissues (including vessels, organ, bone, and so on) [22]. To extract the lung area, the bi-level thresholding technique was applied using an optimal threshold to get a binary image. An example of the thorax image and the bi-level threshold output can be shown in Fig. (12.a), and Fig. (12.b). A median filter of size 9*9 was applied to the binary image to leave just the two lungs (Fig.(12.c)). Then, the mathematical morphological operation was applied to the output binary image; first the closing morphological operation was applied using a structural element disk shape of size 3 to smooth the outer lung contour. After closing, the lungs area in the resulting binary image have holes due to the removal of the pixels representing the pulmonary vessels and nodules which are filled using a filling operation. Examples of a closed and filled image can be shown in Fig. (12.d) and Fig. (12.e). The next step was to apply an opening operation employing a structural element of diamond of size 1 to remove any extra pixels (Fig. (12.f)). As shown in the thoracic contour construction, the construction of lung contours is performed by closing the on regions in the resulting binary image. All pixels in the original gray level preprocessing image that lie within this contour compose the segmented lung regions, whereas pixels outside this contour are removed. So the final step after suppressing unwanted pixels, the image obtained was multiplied with the gray level thorax image to get the segmented lungs in the CT chest images Fig. (12.g).

3.3 Extraction of Nodule candidates

The main objective of this step is to obtain a typical extraction of regions of interest (ROIs) that composed of the nodule candidates using the bi-level threshold technique. By choosing an appropriate threshold, accurate nodule candidates extraction can be obtained which include solid, part-solid, and non-solid pulmonary nodules. A median filter of size 5*5 was applied to the binary image to remove any unwanted isolated pixels. Finally the image obtained is

multiplied with gray level lung image to get the ROIs in the CT chest images. Fig.13 shows the ROIs obtained.

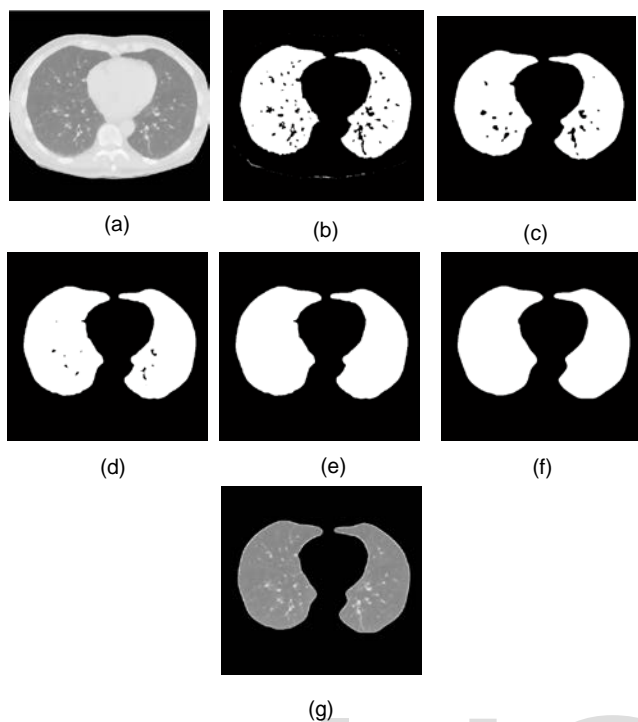


Fig 12: The steps of lungs segmentation technique (a) The segmented thorax image, (b) The binary image, (c) The filtered image, (d) The dilated image, (e) The filled image, (f) The closed image, (g) The segment lungs image.

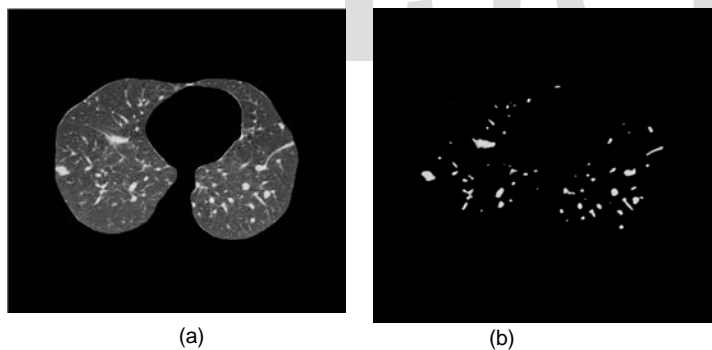


Fig 13: (a) The segmented lung image , (b) The detected ROIs

3.4 Performance Evaluation

To evaluate the performance of the proposed framework, the resulted area were compared with those obtained by three different techniques. These techniques are Otsu thresholding [25], local entropy-based transition region extraction and thresholding [26], and the basic global thresholding [25]. Fig.14 shows the ROIs that obtained by use the four different thresholding techniques. Two criteria were utilized to provide a quantitative comparison. These are the edge mismatch and the region non-uniformity [27].

3.4.1 Edge Mismatch

In this criteria, a comparison between the different histogram thresholding techniques was performed by first applying the edge map obtained from the thresholded image to the gray

level lung image and comparing the resulted images to identify the best techniques that accommodate all ROIs area [27]. Fig.15 and Fig.16 shows the results of the application of the edge mismatch criteria to the four different segmented images result from four different histogram thresholding techniques.

3.4.2 Region Non-uniformity

Region non-uniformity is defined as:

$$NU = \frac{|F_T|}{|F_T + B_T|} \frac{\sigma_f^2}{\sigma^2} \quad (5)$$

where σ^2 is the whole image variance, and σ_f^2 represents the foreground variance, B_T and F_T denote the background and foreground area pixels in the segmented image [27]. According to a non-uniformity (NU) measure the segmented image of smallest NU measure is the best histogram thresholding technique. The calculated non-uniformity measures of each segmented image for all applied histogram thresholding techniques are shown in Table 1.

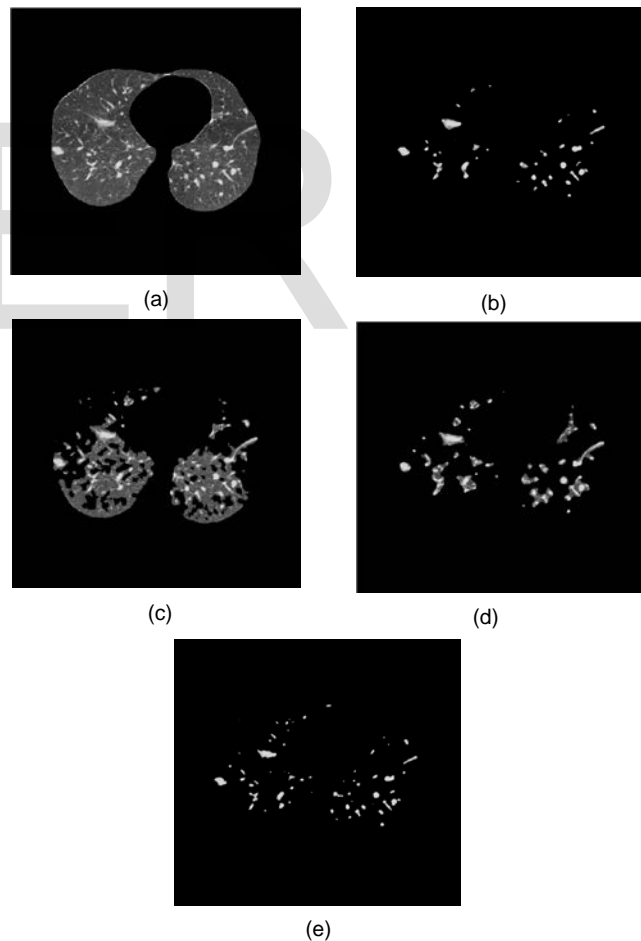
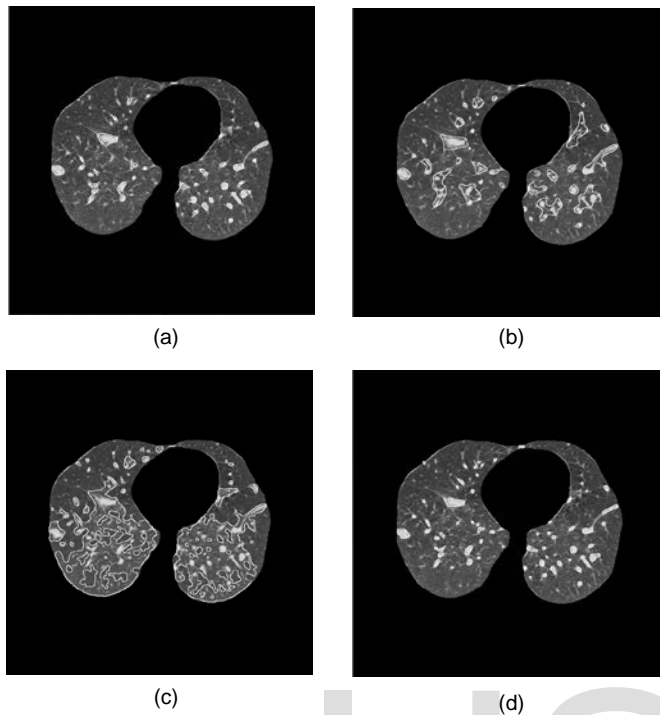


Fig 14: (a) The segmented lung image , (b) ROIs using Otsu's method, (c) ROIs using Local Entropy-Based Transition Region, (d) ROIs using Basic Global Thresholding, and (e) ROIs using the proposed framework.



(b) Local entropy-based transition region extraction thresholding technique, (c) Basic global thresholding technique, and (d) the proposed framework.

TABLE 1: THE NU MEASURE CALCULATED FOR THE SEGMENTED IMAGES USING ALL APPLIED HISTOGRAM

The Histogram Thretholding Technique	NU
Otsu thresholding technique	0.0225
Local entropy-based transition region extraction thresholding technique	0.1533
basic global thresholding technique	2.2029
proposed framework	0.0188

By visual comparison of the images in Fig.15 and comparing the results tabulated in Table 1 shows that the proposed framework gives the highest accuracy to detect the pulmonary nodule candidates.

4 Conclusion

The present work is concerned with the development of an accurate and low computational automatic segmentation framework for the extraction of the human's lung and the detection of the pulmonary nodule candidates in CT chest scan images. The framework started with preprocessing the CT chest images to enhance the image contrast and noise reduction using a Wiener filter which gives the best denoised CT images.

An automatic lung segmentation step and an automatic

pulmonary nodules candidates extraction step were followed that are based on the determination of an optimal gray-level threshold using the analysis of a diagonal histogram of the pixels of the CT scan images. The performance of the segmentation framework was assessed using a number of standard Computed Tomographic (CT) images available through an early lung cancer action project (ELCAP) association. The results were compared with those obtained from other three previously published algorithms and showed that the proposed framework gives the highest accuracy and helps to increase the speed of the Computer-Aided Detection (CAD) systems.

REFERENCES

1. JP. Ko, DP. Naidich, "Computer-aided diagnosis and the evaluation of lung disease", *J Thorac Imaging*, 2004;19(3):136-155.
2. Y. Zhiwei, H. Zhengbing, L. Xudong, Ch. Hongwei, "Image Segmentation Using Thresholding and Swarm Intelligence", *JOURNAL OF SOFTWARE*, VOL. 7, NO. 5, MAY 2012.
3. S. Mukhopadhyay, "A Segmentation Framework of Pulmonary Nodules in Lung CT Images", *J Digit Imaging* (2016) 29:86-103.
4. T. Manikandan, N. Bharathi, "A Survey on Computer-Aided Diagnosis Systems for Lung Cancer Detection", *International Research Journal of Engineering and Technology (IRJET)*, Volume: 03 Issue: 05, May-2016.
5. S. Parveen, C. Kavitha, "A REVIEW ON COMPUTER AIDED DETECTION AND DIAGNOSIS OF LUNG CANCER NODULES", *International Journal of Computers & Technology*, Volume 3 No. 3, Nov-Dec, 2012.
6. A. Mansoor, U. Bagci, B. Foster, Xu. Ziyue, G.Z. Papadakis, L.R. Folio, J.K. Udupa, D.J. Mollura, "Segmentation and Image Analysis of Abnormal Lungs at CT: Current Approaches, Challenges, and Future Trends", *Radio Graphics* 2015; 35:1056-1076.
7. X. Ye, X. Lin, J. Dehmeshki, G. Slabaugh, G. Beddoe, "Shape-based computer-aided detection of lung nodules in thoracic CT images", *IEEE Trans. Biomed. Eng.* 2009, 56, 1810-1820.
8. Y. Lee, T. Hara, H. Fujita, S. Itoh, T. Ishigaki, "Automated detection of pulmonary nodules in helical CT images based on an improved template-matching technique", *IEEE Trans. Med. Imaging*, 2001, Vol. 20, pp.595-604.
9. M. Evelina, "Algorithms for automatic detection of lung nodules in CT scans", *IEEE International Workshop on Medical Measurement and Applications, MEMEA*, 2011
10. A. Roozgard, "Malignant Nodule Detection on Lung CT Scan Images with Kernel RX algorithm", *proc. IEEE-EMBS International Conference on Biomedical and Health Informatics*, pp.499-502, 2012.
11. L. Daw-Tung, Y. Chung-Ren, C. Wen-Tai, "Autonomous detection of pulmonary nodules on CT images with a neural network-based fuzzy system", *Computerized Medical Imaging and Graphics* 29 (2005) 447-458.
12. Early Lung Cancer Action Program (ELCAP), available from: <http://www.via.cornell.edu/lungdb.html>. [Last cited on 2011 Dec 05].
13. T. Acharya, A.K. Ray, "Image Processing: Principles and Applications", *Wiley-Interscience* 2005.
14. S.M. Pizer, E.P. Amburn, R. Cromarte, K. Zuiderveld, "Adaptive Histogram Equalization and its variations", *Computer vision graphics, and image processing* Vol. 39, Issue: 3, pp. 355-368, 1987.
15. W.K. Pratt, *Digital Image Processing*, 3rd Edition, A Wiley-Interscience Publication. ISBNs: 0-471-22132-5, New York, 2001.
16. S. Asadi, H. Hassanpour, A. Akbar Pouyan, "Texture Based Image Enhancement using Gamma Correction", *Middle East Journal of Scientific*

- Research, Vol. 6, No. 6, 2010.
17. Z. Al-Ameen, G. Sulong, M. Gapar, M. Johar, "Enhancing the Contrast of CT Medical Images by Employing a Novel Image Size Dependent Normalization Technique", *International Journal of Bio-Science and Bio-Technology* Vol. 4, No. 3, September, 2012.
 18. C. Gonzales C., E. Woods, "Digital Image Processing," 2nd Edition, New Jersey, Prentice Hall, 2004.
 19. A. Tinku, K. Ajoy, "Image Processing Principles and applications," John Wiley & Sons, Inc., Hoboken, New Jersey, 2005.
 20. F.E. Abou-Chadi, H.M. Amer, M.I. Obayya, " A Computer-Aided System for Classifying Computed Tomographic (CT) Lung Images Using Artificial Neural Network and Data Fusion", *International Journal of Computer Science and Network Security*, VOL.11 No.10, October 2011.
 21. S.G. Armato, H. MacMahon, " Automated lung segmentation and computer-aided diagnosis for thoracic CT scans", *International Congress Series* 1256 (2003) 977-982
 22. L. Daw-Tung, Y. Chung-Ren, C. Wen-Tai, "Autonomous detection of pulmonary nodules on CT images with a neural network-based fuzzy system", *Computerized Medical Imaging and Graphics* 29 (2005) 447-458.
 23. R.S. Joao, C.S. C.Z. Aristofanes, C.P. Anselmo, A.N. Rodolfo, " Methodology for automatic detection of lung nodules in computerized tomography images", *computer methods and programs in biomedicine* 98 (2010) 1-14.
 24. E.B. Ayman, E. Ahmed, A.E. Mohamed, G.F. Georgy, F. Robert, F. Aly, "Automatic Detection of 2D and 3D Lung Nodules in Chest Spiral CT Scans", *International Journal of Biomedical Imaging* Volume 2013, Article ID 517632, 11 pages.
 25. D.R. Raju, Neelima, "Image Segmentation by using Histogram Thresholding", *IJCSET*, January, 2012 Vol 2, Issue 1, 776-779.
 26. C. Yan, N. Sang, T. Zhang, " Local entropy-based transition region extraction and thresholding", *Pattern Recognition Letters* 24 (2003) 2935-2941.
 27. M. Sezgin, B. Sankur, " Survey over image thresholding techniques and quantitative performance evaluation", *Journal of Electronic Imaging* 13(1), 146-165 (January 2004).